

Switching Energy of Ferromagnetic Logic Bits

Behtash Behin-Aein, Sayeef Salahuddin, and Supriyo Datta, *Fellow, IEEE*

Abstract

Power dissipation in switching devices is believed to be the single most important roadblock to the continued downscaling of electronic circuits. There is a lot of experimental effort at this time to implement switching circuits based on magnets and it is important to establish power requirements for such circuits and their dependence on various parameters. This paper analyzes switching energy which is dissipated in the switching process of single domain Ferromagnets used as *casca*dable logic bits. We obtain generic results that can be used for comparison with alternative technologies or guide the design of magnet based switching circuits. Two central results are established. One is that the switching energy drops significantly if the ramp time of an external pulse exceeds a critical time. This drop occurs more rapidly than what is normally expected of adiabatic switching for a capacitor. The other result is that under the switching scheme that allows for logic operations, the switching energy can be described by a single equation in both fast and slow limits. Furthermore, these generic results are used to quantitatively examine the possible operation frequencies and integration densities of these logic bits which show that nanomagnets can have scaling laws similar to CMOS technology.

Index Terms

switching energy, nanomagnet, casca

dable logic, Landau-Lifshitz-Gilbert equation (LLG), MQCA, fast pulse, adiabatic pulse, critical ramp time

I. INTRODUCTION

It has been suggested [1] that the use of collective systems like a magnet can reduce the switching energy significantly compared to that required for individual spins. There is also a lot of experimental effort [2]–[7] at this time to implement switching circuits based on magnets. There has been some work [8] on modeling magnetic circuits like MQCA's in the atomic scale using quantum density matrix equation but most of the work [9]–[13] is in the classical regime using the well known micromagnetic simulators (OOMMF) based on the Landau-Lifshitz-Gilbert (LLG) [15]–[17] equation. This paper too is based on the LLG equation, but our focus is not on obtaining the energy requirement of any specific device in a particular simulation. Rather it is to obtain generic results that can guide the design of magnet based switching circuits as well as providing a basis for comparison with alternative technologies.

The results we present are obtained by analyzing the casca

dable switching scheme illustrated in Fig.1 where the magnet to be switched (magnet 2) is first placed along its hard axis by a magnetic pulse (see 'mid state' in Fig.1). On removing the pulse, it falls back into one of its low energy states (up or down) determined by the 'bias' provided by magnet 1. What makes this scheme specifically suited for logic operations is that it puts magnet 2 into a state determined by magnet 1 (thereby transferring information), but the energy needed to switch magnet 2 comes largely from the external pulse *and not from magnet 1*. This is similar to conventional electronic circuits where the energy needed to charge a capacitor comes from the power supply, although the information comes from the previous capacitors. This feature seems to be an essential ingredient needed to *casca*de logic units. To our knowledge, the switching scheme shown in Fig.1 was first discussed by Bennett [18] and is very similar to the schemes described in many recent publications (see e.g Likharev et.al [19], Kummamuru et.al [20] and Csaba et.al [9]).

This paper uses the LLG equation to establish two central results. One is that the switching energy drops significantly as the ramp time τ_r of the magnetic pulse exceeds a critical time τ_c given by

$$\tau_c = \frac{(1 + \alpha^2)}{2\alpha(|\gamma|H_c)} \quad (1)$$

where γ is the gyromagnetic ratio of electron, α is the Gilbert damping constant, and $H_c = \frac{2Ku_2}{M_s}$ is the minimum magnitude of the pulse needed to place the magnet along its hard axis. Ku_2 (anisotropy energy per unit volume) and M_s (saturation magnetization) are the two basic parameters characterizing any single domain spherical magnet with magnetocrystalline uniaxial anisotropy. This is similar to the drop in the switching energy of an RC circuit when $\tau_r \gg RC$. But the analogy is only approximate since the switching energy for magnets drops far more abruptly with increasing τ_r . The significance of τ_c is that it tells us how slow a pulse needs to be in order to qualify as "adiabatic" and thereby reduce dissipation significantly. (see section §VI for typical values of material parameters, switching fields, switching frequencies, etc).

Interestingly, we find that the switching energy for the trapezoidal pulses investigated in this paper in both the 'fast' and 'slow' limits can be described by a single equation which is the other central result of this paper

$$E_d = \left(\frac{\tilde{H}}{H_c} \right)^P (2Ku_2V) \quad (2)$$

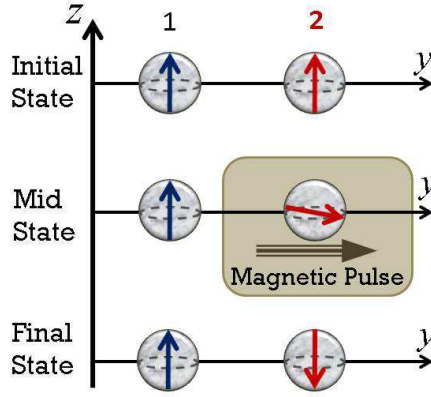


Fig. 1. A magnetic pulse is applied to magnet 2, provides energy and places it along its hard axis (along y) where a small bias field due to magnet 1 can tilt it upwards or downwards thereby dictating its final state on removing the pulse.

In the fast limit, \tilde{H} is the magnitude of the pulse while in the slow limit, \tilde{H} is related to the magnitude of the small bias field [21]. p is a parameter in the range $1 \leq p \leq 2$. Ku_2V (V is the volume) is the height of the anisotropy energy barrier separating the two stable states of the magnet, and has to be large enough so that the magnet retains its state while computation is performed without thermal fluctuations being able to flip it. The retention time for a given Ku_2V can be calculated using [22]–[24] $\tau = \tau_0 e^{\frac{Ku_2V}{kT}}$ where τ_0^{-1} is the attempt frequency with the range $10^9 - 10^{12} s^{-1}$ [23], [25] which depends in a nontrivial fashion on variables like anisotropy, magnetization and damping.

Later in this paper (§VI-A and §VI-B) we will show with simple examples how equations 1 and 2 can be used to choose magnet parameters (Ku_2 , V , M_s) in order to optimize switching energy and speed not just for individual magnets (Fig.1) but for magnet based switching circuits like a chain of inverters (Fig.9). Furthermore these equations can be used to compare magnet based switching circuits with alternative technologies.

It has to be emphasized that dissipation of the external circuitry also has to be evaluated for any new technology. A careful evaluation would require a consideration of actual circuitry to be used (see e.g. [13], [14]) and is beyond the scope of this paper. However following Nikonov et.al. [14], if a wire coil is used to produce the pulse, we can estimate the energy dissipated in creating the field H_{pulse} as $\frac{H_{pulse}^2 V}{2Q}$ in CGS system of units. Q is the quality factor of the circuit and V is the volume over which the field extends. Depending on Q , V and H_{pulse} the dissipated energy can be much larger, comparable to or much smaller than Ku_2V which sets the energy scale for the effects considered here in this paper.

Overview of the paper: As mentioned before our results are based on direct numerical simulation of the LLG equation. However we find that in two limiting cases, it is possible to calculate switching energy simply using the energetics of magnetization and these limiting results are described in sections §II (dissipation with fast pulse) and §III (dissipation with adiabatic pulse) which are related to equation 2. In §IV we use the LLG equation to show that the switching energy drops sharply for ramp times larger than the critical time given by equation 1. In section §V using coupled LLG equations we analyze a chain of inverters to show that the total dissipation increases linearly with the number of nanomagnets thus making it reasonable to use the one-magnet results in our paper to evaluate complex circuits, at least approximately. Finally in section §VI possible operation frequencies and integration densities are evaluated in the light of these results.

II. DISSIPATION WITH FAST ($\tau_r \ll \tau_c$) PULSE

There are two magnetic fields that control the switching (see Fig.1): The external pulse and the bias field due to the neighboring magnet. In section §II-A we show that the switching energy with infinitesimal bias field is related to the magnitude of the external pulse by

$$E_d = \left(\frac{H_{pulse}}{H_c} \right)^2 (2Ku_2V) \quad \text{for } H_{pulse} \leq H_c \quad (3a)$$

$$E_d = 2Ku_2V \quad \text{for } H_{pulse} = H_c \quad (3b)$$

$$E_d = \left(\frac{H_{pulse}}{H_c} \right) (2Ku_2V) \quad \text{for } H_{pulse} \geq H_c \quad (3c)$$

In practice a bias field H_{dc} is needed to overcome noise and variability. However we will show in §II-B that for $H_{dc} \leq 0.1H_c$, dissipation can still be calculated using equation 3.

Before we get into the discussion of switching energy, let us briefly review the energetics of a magnet. The energy of a

spherical magnet with second order magnetocrystalline uniaxial anisotropy can be described by $\frac{E}{V} = Ku_2 \sin^2(\theta)$ where θ measures the deflection from the easy axis which we take as the z axis. All isotropic terms have been omitted because they have no bearing on dynamics and hence dissipation of the magnet [26]. If an external magnetic field H_{pulse} and a bias field H_{dc} are exerted on the magnet, then the energy equation reads

$$\frac{E}{V} = -M_s \hat{m} \cdot \vec{H}_{pulse} + Ku_2 \sin^2(\theta) - M_s \hat{m} \cdot \vec{H}_{dc}$$

M_s is the magnetic moment per unit volume also called saturation magnetization. \hat{m} is a unit vector in the direction of magnetization. V is the volume of the magnet and Ku_2 is the second order anisotropy constant with dimensions of energy per unit volume. The applied field H_{pulse} is along the hard axis y , the bias field H_{dc} is along the easy axis z so the energy equation becomes

$$\frac{E}{V} = -M_s H_{pulse} \sin(\theta) \sin(\phi) + Ku_2 \sin^2(\theta) - M_s H_{dc} \cos(\theta) \quad (4)$$

We are interested in the initial and final state energies for which $\phi = 90^\circ$ i.e. magnetization is in the $y - z$ plane.

A. Zero bias field ($H_{dc} = 0$)

Fig.2 is plotted using equation 4 with $\phi = 90^\circ$ and $H_{dc} = 0$ which is the first case to be discussed. The different contours correspond to different values of H_{pulse} .

Derivation of equation 3b: Let's start with equation 3b which is the most important and also easiest. Dissipation occurs both during turn-on and turn-off of the pulse and the overall switching energy is sum of the two in general. The dashed contour in Fig.2 corresponds to $H_{pulse} = H_c$ which is the minimum value needed to make $\theta = 90^\circ$ (point 2) the energy minimum. For a pulse with fast ($\tau_r \ll \tau_c$) *turn-on*, dissipation can be calculated using equation 4 as the difference between the initial and the final energies which are given by point 1 (or 4) and point 2 on the dashed contour. This value is

$$E_{1(4)} - E_2 = Ku_2 V$$

For a pulse with fast ($\tau_r \ll \tau_c$) *turn-off*, the energy contour immediately changes from the dashed one to the uppermost one in Fig.2. Under any infinitesimal bias, magnetization falls down the barrier to the left (relaxing to point 1) or to the right (relaxing to point 4) giving a dissipation of

$$E_3 - E_{1(4)} = Ku_2 V$$

equal to the turn-on dissipation. The switching energy (*total dissipation*) is sum of the values for turn-on and turn-off which gives us equation 3b.

Derivation of equation 3c: This is the case with $H_{pulse} > H_c$. The bottom most energy contour in Fig.2 shows such a situation as an example. The minimum of energy is still at $\theta = 90^\circ$ (point 5) however now the energy well is deeper. For a pulse with fast ($\tau_r \ll \tau_c$) *turn-on*, dissipation is the difference between the initial and final state energies

$$E_{1(4)} - E_5 = (M_s H_{pulse} - Ku_2) V$$

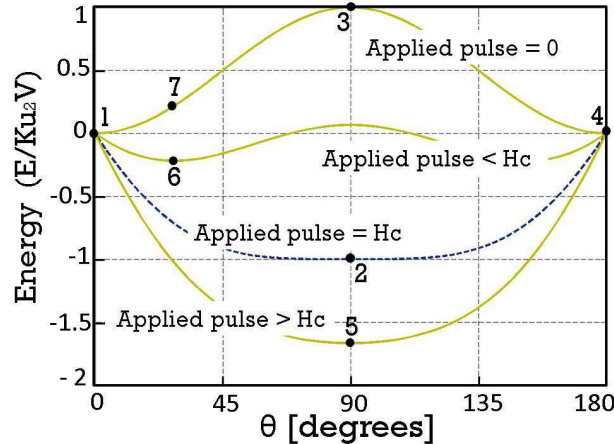


Fig. 2. Energy landscape of the magnetization under various applied fields. For fast turn-on of the pulse to H_c , dissipation is equal to the barrier height (magnet relaxes from point 1 (or 4) to point 2). When the field is turned off fast, magnet relaxes from point 3 to point 4 or 1 depending on any infinitesimal bias again dissipating an amount equal to the barrier height.

(Where E_5 is used as a generic notation for the bottom of the well with $H_{pulse} > H_c$). For a pulse with fast ($\tau_r \ll \tau_c$) *turn-off*, the energy contour immediately changes from the bottom most curve to the uppermost curve in Fig.2. Depending on any infinitesimal bias magnet will relax from point 3 to either point 1 or 4 dissipating the difference

$$E_3 - E_{1(4)} = Ku_2V$$

The switching energy is sum of the values for turn-on and turn-off which with straightforward algebra gives us equation 3c.

Derivation of equation 3a: With $H_{pulse} < H_c$, magnetization will not align along its hard axis ($\theta = 90^\circ$). This can be seen in Fig.2 where for a pulse lower than H_c there are two minima of energy not located along the hard axis. Depending on the initial conditions and noise, magnetization will end up in one of the two minima with no control. Nevertheless we derive dissipation for these pulses because we use the results in section §III-A to show switching energy in the adiabatic limit. For a pulse with fast ($\tau_r \ll \tau_c$) *turn-on*, dissipation is the difference between the initial and final state energies

$$E_1 - E_6 = \left(\frac{M_s H_{pulse}}{2Ku_2} \right)^2 (Ku_2V) \quad (5)$$

For a pulse with fast ($\tau_r \ll \tau_c$) *turn-off*, the energy contour suddenly becomes the uppermost one in Fig.2. At that moment magnetization is still at the same θ (point 7). It follows down the barrier with the dissipation given by

$$E_7 - E_1 = \left(\frac{M_s H_{pulse}}{2Ku_2} \right)^2 (Ku_2V) \quad (6)$$

The *total dissipation* is sum of the values for turn-on and turn-off which gives us equation 3a.

B. Non-zero bias field ($H_{dc} \neq 0$)

In this section we show that for $H_{pulse} = H_c$, so long as $H_{dc} \leq 0.1H_c$ switching energy can be calculated fairly accurately using equation 3b considering only the effect of H_{pulse} . For $H_{pulse} > H_c$ the effect of H_{dc} is even less pronounced as compared to H_{pulse} and equation 3c can be used to calculate dissipation. Again we are interested in initial and final state energies which can be calculated using equation 4 with $\phi = 90^\circ$. H_{dc} can be positive (along z) or negative (along $-z$). Fig.3

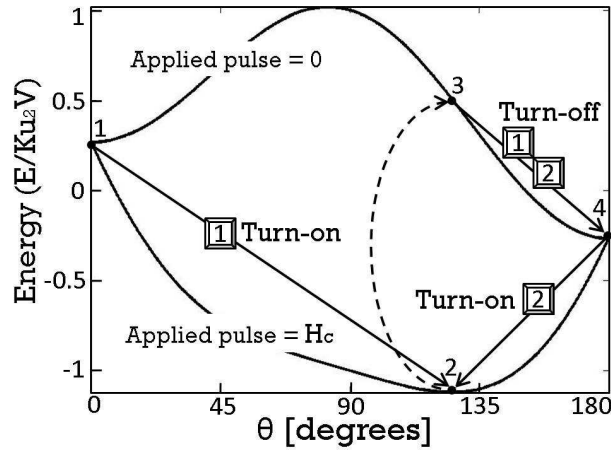


Fig. 3. Energy landscape of magnetization with bias field H_{dc} in the $-z$ direction for two values of the pulse: 0 and H_c . Upon *turn-on*, if magnetization starts from $\theta = 0^\circ$ (*case 1*), it drops from point 1 ($E = +M_s V H_{dc}$) to point 2 dissipating the difference. If it starts from $\theta = 180^\circ$, it drops from point 4 ($E = -M_s V H_{dc}$) to point 2 dissipating the difference. Upon *turn-off*, both cases 1 and 2 drop from point 3 to point 4 dissipating the difference.

shows the energy landscape with an H_{dc} in the $-z$ direction. If $H_{dc} \neq 0$ then the up and down states (points 1 and 4) of the magnet have different initial energies which result in two different cases to be analyzed. *Case 1* designates the situation where initial magnetization (point 1) and H_{dc} are in the *opposite* direction. *Case 2* designates the situation where initial magnetization (point 4) and H_{dc} are in the *same* direction.

For a pulse with fast ($\tau_r \ll \tau_c$) *turn-on*, *case 1* dissipates the difference between points 1 and 2 and *case 2* dissipates the difference between points 4 and 2. When the pulse is suddenly turned off, in both cases magnetization finds itself at point 3, drops down to point 4 and dissipates the difference. It is not possible to give an exact closed form expression for the value of dissipation with non-zero bias. Instead based on numerical calculations, we show figures that provide useful insight to conclude that for pulses with fast ramp time the effect of bias on switching energy is negligible.

The energy of point 2 (and subsequently point 3) depicted in Fig.3 changes as the relative magnitude of H_{dc} and H_c are changed. We like to know how dissipation changes as a function of the ratio $\frac{H_{dc}}{H_c}$. The numerical results are plotted in Fig.4 using equation 4. Fig.4a shows that for a pulse with fast *turn-on* and small values of $\frac{H_{dc}}{H_c}$, both cases dissipate about Ku_2V . As

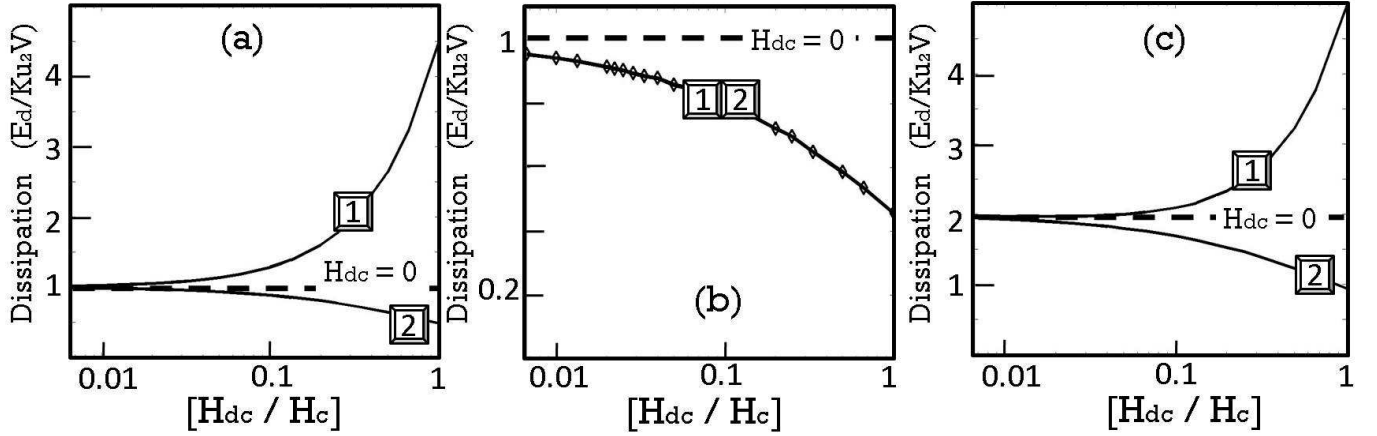


Fig. 4. (a) Shows the *turn-on* dissipation with non-zero bias. Cases 1 and 2 correspond to different initial directions of magnetization (see Fig.3). The dashed line depicts the value of dissipation with zero bias. (b) Shows the *turn-off* dissipation with non-zero bias. Both cases 1 and 2 dissipate the same amount (see Fig.3). (c) Shows the total dissipation with non-zero bias. Notice that for relevant (small) values of $\frac{H_{dc}}{H_c}$, total dissipation of both cases 1 and 2 is close to the value $2Ku_2V$ which is the same as the case with infinitesimal bias.

this ratio is increased, the energy separation between points 1 and 2 (see Fig.3) increases and that of points 4 and 2 decreases which results in higher dissipation of *case 1* and lower dissipation of *case 2*. Fig.4b shows the dissipation for a pulse with fast *turn-off* which is less than the barrier height Ku_2V and is expected because under the presence of H_{dc} , after turn-on, magnetization ends up closer to the final state (see Fig.3) as compared to the case where $H_{dc} = 0$ (see Fig.2). The switching energy is sum of the dissipation values for turn-on and turn-off plotted in Fig.4c. For $H_{dc} = H_c$ the bias field H_{dc} alone can switch the magnet and it is completely an unwanted situation [27]. Note that for practical purposes, values of H_{dc} are small compared to H_c (for instance $H_{dc} \leq 0.1H_c$) and the switching energy is more or less about $2Ku_2V$ which gives us equation 3b. For $H_{pulse} > H_{dc}$ the effect of bias is even less pronounced and switching energy can be calculated using equation 3c.

III. DISSIPATION WITH ADIABATIC ($\tau_r \gg \tau_c$) PULSE

We have seen in section §II that for pulses with fast ramp times, the effect of bias (H_{dc}) is negligible for $H_{dc} \leq 0.1H_c$ and switching energy is obtained fairly accurately even if we set $H_{dc} = 0$. By contrast for pulses with slow ramp time, switching energy can be made arbitrarily small for $H_{dc} = 0$ and the actual switching energy is determined entirely by the H_{dc} that is used. In this section we will first show why the switching energy can be arbitrarily small for $H_{dc} = 0$ and then show that for $H_{dc} \neq 0$ it will saturate in *case 1* but can be made arbitrarily small in *case 2* [28]:

$$E_d = \left(\frac{2H_{dc}}{H_c} \right)^p (2Ku_2V), \quad (\text{case 1: } H_{dc} \text{ and initial magnetization in the opposite direction}) \quad (7)$$

$$E_d \rightarrow 0, \quad (\text{case 2: } H_{dc} \text{ and initial magnetization in the same direction}) \quad (8)$$

A. Zero bias field ($H_{dc} = 0$)

Gradual *turn-on* of the pulse corresponds to increasing the pulse in many small steps. Fig.5a shows the energy landscape. As the field is gradually turned-on the energy contours change little by little from top to bottom. The minimum of energy gradually shifts from point 1 (or 4) to point 2. Magnetization hops from one minimum of energy to the other. But why is it that gradual turn-on of the pulse dissipates less than sudden turn-on?

If the external pulse is turned on to H_c in N steps, total dissipation is N times the dissipation of each step. We show that dissipation of each step is proportional to $\frac{1}{N^2}$; hence as the number of steps increases, dissipation decreases as $\frac{1}{N}$ and in the limit of $N \rightarrow \infty$, $E_d \rightarrow 0$ (this is not unlike a similar argument that has been given for charging up a capacitor adiabatically [29]). At each step when the pulse is increased by $\Delta H = \frac{H_c}{N}$, the dissipated energy is the difference between initial and final state energies. Such a situation is illustrated in Fig.5a where a denotes a minimum on an energy contour corresponding to H_n (magnitude of the pulse after n steps). When the pulse is stepped up to H_{n+1} , magnetization suddenly finds itself at point b (initial state) and falls down to c (final state). Note that dissipation is $E_b - E_c$ and not $E_a - E_c$. This is because when the field suddenly changes from H_n to H_{n+1} , magnet has not had time to relax and dissipate energy. Here we use E_b and E_c as generic notations for initial and final energy of each step. E_b can be found by finding the θ which corresponds to point a (the minimum of energy with $H_{pulse} = H_n$) and substituting it in equation 4 with $H_{pulse} = H_{n+1}$. With straightforward algebra we get $E_b = -(M_s V)H_{n+1} \left(\frac{M_s H_n}{2Ku_2} \right) + (Ku_2V) \left(\frac{M_s H_n}{2Ku_2} \right)^2$. Equation 5 can be used to calculate $E_c = - \left(\frac{M_s H_{n+1}}{2Ku_2} \right)^2 (Ku_2V)$.

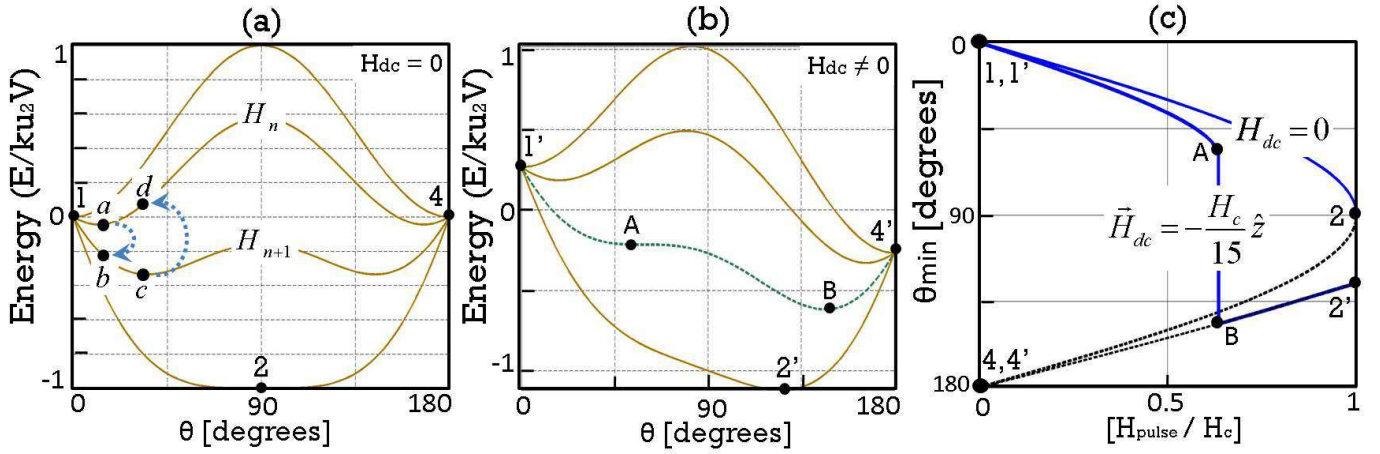


Fig. 5. (a) Energy landscape of magnetization as pulse is increased from 0 (top curve) to H_c (bottom curve) with $H_{dc} = 0$. (b) Energy landscape of magnetization as pulse is increased from 0 (top curve) to H_c (bottom curve) with $H_{dc} \neq 0$ in the $-z$ direction. (c) Adiabatic progression of ground state in the presence of a bias field H_{dc} in the $-z$ direction. Figure shows those values of θ which minimize energy as the pulse is adiabatically ramped from 0 to 1 and back to 0.

Using the identities $H_{n+1} = H_n + \Delta H$ and $\Delta H = \frac{H_c}{N}$, the dissipated energy per step is obtained as

$$E_d^{step} = E_b - E_c = Ku_2V \left(\frac{1}{N^2} \right)$$

For gradual *turn-off* consider points c, d and a . When $H_{pulse} = H_{n+1}$, magnetization is at c and after the pulse is decreased by one step to H_n , it finds itself at d , falls down to a dissipating the difference $E_d - E_a$. E_d can be found by finding the θ which corresponds to point c (the minimum of energy with $H_{pulse} = H_{n+1}$) and substituting it in equation 4 with $H_{pulse} = H_n$. We get $E_d = -(M_s V) H_n \left(\frac{M_s H_{n+1}}{2Ku_2} \right) + (Ku_2V) \left(\frac{M_s H_{n+1}}{2Ku_2} \right)^2$. Again equation 5 can be used to give $E_a = - \left(\frac{M_s H_n}{2Ku_2} \right)^2 (Ku_2V)$. Using the identities $H_{n+1} = H_n + \Delta H$ and $\Delta H = \frac{H_c}{N}$, we obtain for the dissipated energy per step

$$E_d^{step} = E_d - E_a = Ku_2V \left(\frac{1}{N^2} \right)$$

The switching energy is sum of the dissipation values for *turn-on*: $E_d = \frac{Ku_2V}{N}$ and *turn-off*: $E_d = \frac{Ku_2V}{N}$ which in the limit of $N \rightarrow \infty$, tends to 0 ($E_d \rightarrow 0$).

B. Non-zero bias field ($H_{dc} \neq 0$)

For *turn-on* let's consider *case 1* first where initial magnetization and H_{dc} are in opposite directions (point $1'$ in Fig.5b). As the field is gradually turned-on, magnetization starts from point $1'$ and hops from one minimum of energy to the next. Increasing the number of steps brings the minima closer to each other so that magnetization stays in its ground state while being switched. However when magnetization gets to point A , situation changes. At that point the energy barrier which formerly separated the two minima on the two sides disappears. Magnetization falls down from point A to B and dissipates the energy difference. This sudden change in the minimum of energy occurs no matter how slow the pulse is turned on and causes the switching energy to saturate so long as $H_{dc} \neq 0$. Quantitatively this can be seen by plotting θ_{min} vs. H_{pulse} (Fig.5c) using equation 4. When the left solid curve is traced from $\theta_{min} = 0$, it is evident that there is a discontinuous jump in the θ_{min} values which minimize energy when the pulse is increases from 0 to H_c in infinitesimal steps. This discontinuity goes away only when $H_{dc} = 0$ (right solid curve). In *case 2*, magnetization starts from point $4'$, i.e. $\theta_{min} = 180^\circ$ (see Fig.5b and c), gets to point B at which there is *no* sudden change of minimum and as the pulse is increased further to H_c , it gradually moves to point $2'$. During *turn-off* in both cases 1 and 2, magnetization gradually moves from (see Fig.5c) point $2'$ to B and then finally to point $4'$ all along staying in its minimum of energy with no discontinuity. Dissipation tends to zero as the pulse is turned off in infinitesimal steps.

In the slow limit the entire dissipation is determined by the energy difference between points A and B , $E_A - E_B$ in Fig.5b. For a given H_{dc} , one has to find that particular value of H_{pulse} for which the local energy maximum in the middle disappears which means that the second derivative of energy with respect to θ must be zero. Since magnetization has been in the minimum of energy while getting to point A , first derivative of energy with respect to θ must also be equal to zero. Under these conditions, the value of θ at A and subsequently E_A can be found using equation 4. E_B can be found as the true minimum of energy from equation 4 where the first derivative of energy with respect to θ is zero but the second derivative is not. What affects $E_A - E_B$ is the relative magnitude of H_{dc} and H_c . It is not possible to give an analytical closed form

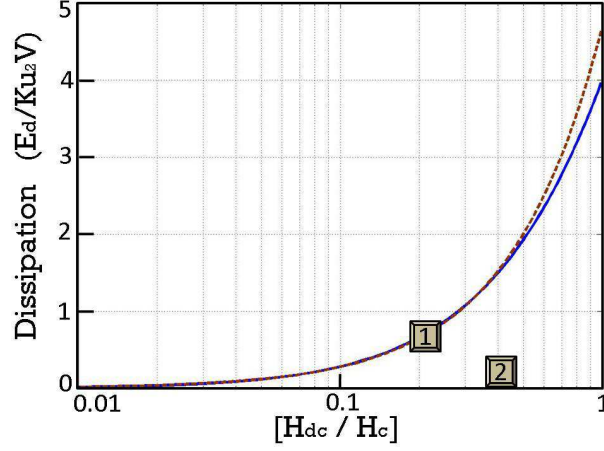


Fig. 6. Shows the total dissipation under adiabatic switching with non-zero bias. There is no dissipation associated with *case 2* and dissipation of *case 1* for small (relevant) values of $\frac{H_{dc}}{H_c}$ is less than the barrier height Ku_2V .

expression for this saturating value of dissipation. Instead we've numerically plotted dissipation versus $\frac{H_{dc}}{H_c}$ (solid curve in Fig.6). For small values of $\frac{H_{dc}}{H_c}$, dissipation can be written as

$$E_d = \left(\frac{2H_{dc}}{H_c} \right)^p (2Ku_2V), \quad (p = 1.23) \quad (9)$$

Where the value of p is obtained by an almost perfect fit to the solid curve for $H_{dc} \leq 0.1H_c$. The dashed curve is plotted using equation 9. As is evident from Fig.6, this equation is fairly accurate. There is some digression from the actual value of dissipation for large values of $\frac{H_{dc}}{H_c}$ which are not of practical interest especially $\frac{H_{dc}}{H_c} = 1$ for which H_{dc} alone can switch the magnet and is completely an unwanted situation [27].

It is important to note that the switching energy in the adiabatic limit is case dependent. For *case 1*, it is given by equation 9 and it is not zero as it might have been expected for dissipation in the adiabatic limit. Interestingly if p was equal to 1, the dissipation would be equal to the energy difference between initial and final states (see points 1' and 4' in Fig.5b). However the actual value is significantly smaller.

IV. MAGNETIZATION DYNAMICS: SINGLE MAGNET

Thus far we've shown switching energy in the two limiting cases of $\tau_r \ll \tau_c$ and $\tau_r \gg \tau_c$. To understand how switching energy changes in between and also how fast it decreases we need to start from the LLG equation which in the Gilbert form reads:

$$\frac{d\vec{M}}{dt} = -|\gamma|\vec{M} \times \vec{H} + \frac{\alpha}{|\vec{M}|}\vec{M} \times \frac{d\vec{M}}{dt} \quad (10)$$

And in the standard form reads:

$$(1 + \alpha^2)\frac{\partial\vec{M}}{\partial t} = -|\gamma|(\vec{M} \times \vec{H}) - \frac{\alpha|\gamma|}{|\vec{M}|}\vec{M} \times (\vec{M} \times \vec{H}) \quad (11)$$

γ is the gyromagnetic ratio of electron and its magnitude is equal to $2.21 \times 10^5(\text{rad.m})(\text{A.s})^{-1}$ in SI and $1.76 \times 10^7(\text{rad})(\text{Oe.s})^{-1}$ in CGS system of units. α is the phenomenological dimensionless Gilbert damping constant. \vec{M} is the magnetization. Here $\vec{H} = \vec{H}_{ani} + \vec{H}_{pulse}$ where $\vec{H}_{ani} = \frac{2Ku_2}{M_s}m_z\hat{z}$. In general \vec{H} can be derived as the overall effective field: $\vec{H} = -\frac{1}{M_sV}\vec{\nabla}_m E$.

The following expressions are all equivalent statements of dissipated power [30], [31]:

$$P_d = \vec{H} \cdot \frac{d\vec{M}}{dt} = \frac{\alpha}{|\gamma||\vec{M}|} \left| \frac{d\vec{M}}{dt} \right|^2 = \frac{\alpha|\gamma|}{(1 + \alpha^2)|\vec{M}|} \left| \vec{M} \times \vec{H} \right|^2 \quad (12)$$

The dissipated power has to be integrated over time to give the total dissipation. In general, LLG can be solved numerically using the Runge-Kutta method. To obtain generic results that are the same for various parameters, we recast LLG and the dissipation rate into a dimensionless form. This will also show the significance of τ_c and demonstrate why for ramp times exceeding $\tau_c = 1$, there is a significant drop in dissipation.

Using scaled variables $\vec{m} = \frac{\vec{M}}{M_sV}$ and $\vec{h} = \frac{\vec{H}}{H_c}$ equation 11 in dimensionless form can be written as

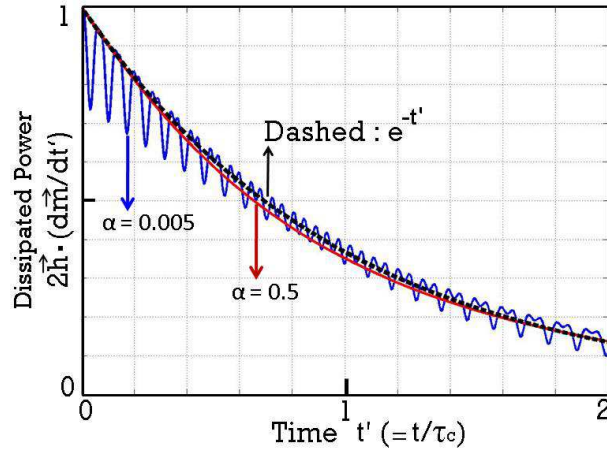


Fig. 7. Solid lines show the dissipated power $2\vec{h} \cdot \frac{d\vec{m}}{dt'}$ under an instantaneous turn-on of H_{pulse} to H_c for $\alpha = 0.005$ and $\alpha = 0.5$. Dashed line shows an exponential decay $e^{-t'}$. This figure shows that although the value of α changes the time (with real dimensions) at which the dissipated power decreases to $1/e$ through changing τ_c , it does not affect the functional form of the decay which is more or less an exponential decay even if α changes by 2 orders of magnitude.

$$\frac{\partial \vec{m}}{\partial t'} = -\frac{1}{2\alpha}(\vec{m} \times \vec{h}) - \frac{1}{2}\vec{m} \times (\vec{m} \times \vec{h}) \quad (13)$$

where $t' = \frac{t}{\tau_c}$ with τ_c given by equation 1. The energy dissipation normalized to Ku_2V can be written as

$$\frac{E_d}{Ku_2V} = \frac{1}{Ku_2V} \int dt \vec{H} \cdot \frac{d\vec{M}}{dt} = \int dt' 2\vec{h} \cdot \frac{d\vec{m}}{dt'} \quad (14)$$

To estimate the time constant involved in switching a magnet it is instructive to plot the integrand $2\vec{h} \cdot \frac{d\vec{m}}{dt'} = \frac{\tau_c}{Ku_2V} \left(\vec{H} \cdot \frac{d\vec{M}}{dt} \right)$ appearing above in equation 14 assuming a step function for H_{pulse} and obtaining the corresponding $\frac{d\vec{m}}{dt'}$ from equation 13. Note that the integrands look much the same for a wide range of α 's from 0.005 to 0.5. All the curves (ignoring the oscillations) can be approximately described by $e^{-t'} = e^{-\frac{t}{\tau_c}}$ thus suggesting that the approximate time constant is τ_c as stated in the introduction.

This is more evident from Fig.8 where we show the energy dissipation for pulses with different ramp times. The dissipated energy drops when τ_r exceeds τ_c as we might expect, but the drop is sharper than an RC circuit. Needless to say, the dissipation values calculated from LLG equation for the two limits of fast pulse ($\tau_r \ll \tau_c$) and adiabatic pulse ($\tau_r \gg \tau_c$) are consistent with the values calculated using energetics previously. Fig.8a shows the *turn-on* dissipation where *case 1* has

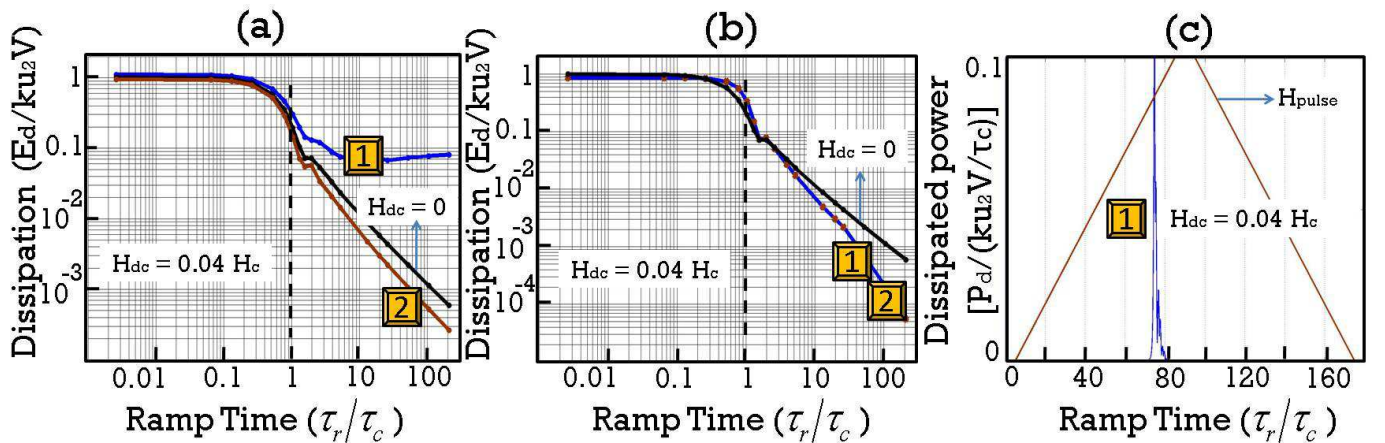


Fig. 8. (a) *Turn-on* dissipation versus ramp time. As ramp time is increased, dissipation in *case 2* decreases arbitrary but it saturates in *case 1*. In both cases there is a significant drop in dissipation once the ramp time exceeds τ_c . (b) *Turn-off* dissipation versus ramp time. In both cases dissipation can be made arbitrarily small by increasing the ramp time. Again there is a significant drop in dissipation as ramp time exceeds τ_c . (c) Dissipated power vs. ramp time. This figure shows that in the slow limit of switching, for *case 1* that has a saturating switching energy, the dissipated power essentially occurs during *turn-on*. This fact was discussed earlier in Fig.5b,c as the dissipation between points A and B during turn-on. If adiabatic limit of switching is really reached, then the dissipated power in this figure will become a very sharp spike.

saturated and *case 2* goes down as ramp time is increased. The curve in the middle is the case with infinitesimal bias $H_{dc} = 0$ and it is just provided for reference. Fig.8b shows the *turn-off* dissipation where both cases 1 and 2 dissipate arbitrarily small amounts as the ramp time is increased. With slow pulses, overall switching energy of *case 2* is very small and the entire switching energy of *case 1* essentially occurs during *turn-on* which is illustrated in Fig.8c. This dissipation was discussed in section §III-B; and it is associated with the sudden fall down from point A to B (see Fig.5b,c). It has a saturating nature and will never become zero. As H_{pulse} is applied more and more gradually, the dissipated power in Fig.8c becomes narrower and taller. In the true adiabatic limit it will become a delta function occurring for one particular value of H_{pulse} .

V. MAGNETIZATION DYNAMICS: CHAIN OF INVERTERS

Fig.9a shows an array of spherical nanomagnets (MQCA) that interact with each other via dipole-dipole coupling [36]. The objective is to determine the switching energy if we are to switch magnet 2 according to the state of magnet 1 [27]. In section §V-A we will show a clocking scheme under which propagation of information can be achieved and basically shows how magnets can be used as *cascadable logic* building blocks. In section §V-B, we briefly go over the method and equations used to simulate the dynamics and dissipation of the coupled magnets. In section §V-C we analyze the dissipation of the chain of inverters where we show that after cascading the magnetic bits, dissipation changes linearly with the number of magnets that the pulse is exerted on. This shows that the switching energy of larger more complicated circuits can be calculated using the one-magnet results presented in this paper at least approximately.

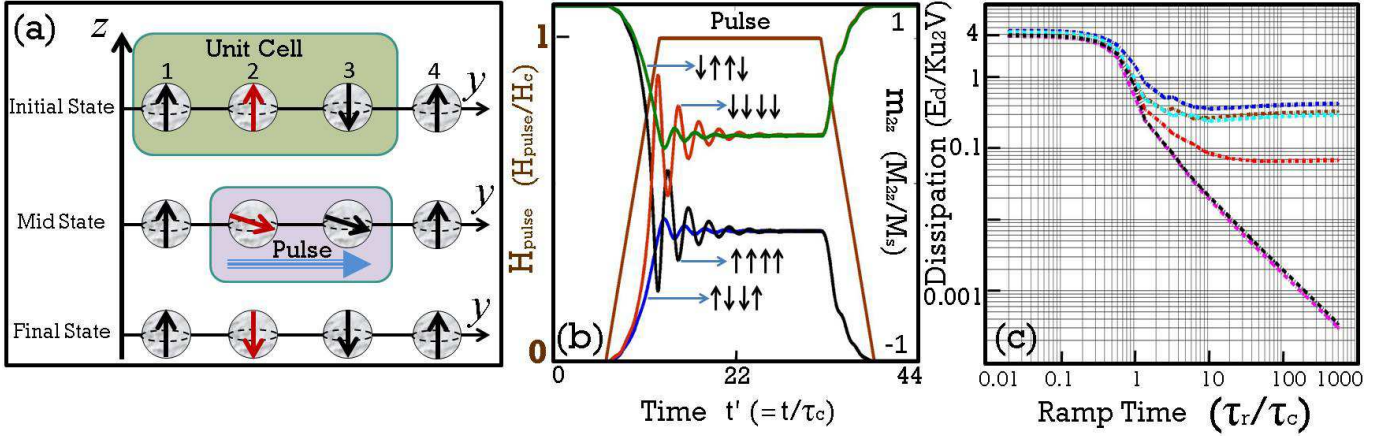


Fig. 9. (a) An array of spherical identical nanomagnets with magnetocrystalline anisotropy and easy axis along z coupled together via dipolar coupling which can be operated as a 3 phase inverter chain. Initially the 4 magnet array can be randomly in any of the 16 possible states. A unit cell is composed of 3 magnets with the real information stored in magnet 1 in the initial state. A y pulse provides energy and puts magnets 2 and 3 in the mid state thereby shutting off the z field of magnet 3 on 2, so that field of magnet 1 can deterministically tilt magnet 2 downwards. Upon removing the pulse, magnet 2 relaxes down in the final state. (b) LIG simulation of coupled system of Fig.9a. This figure shows the proper operation of the clocking scheme by showing the normalized magnetization of magnet 2 along its easy axis for various initial configurations. (c) Dissipation of the array as a function of ramp time. There are $\binom{4}{2} = 6$ physically distinct configurations out of 16 possible states. The dissipation is lower if the initial configuration minimizes the energy of dipolar interaction. Assigning binary 1 to \uparrow and binary 0 to \downarrow the 6 curves (from highest to lowest) represent these configurations: (1)0,15 (2)1,7,8,14 (3)3,12 (4)2,4,11,13 (5)6,9 (6)5,10

A. Clocking scheme

In the introduction we mentioned that in the clocking scheme the role of the clock field is to provide energy whereas field of another magnet acts as a guiding input. Using a clock we can operate an array of exactly similar magnets as a chain of inverters. Fig.9a shows a 3 phase inverter chain where the unit cell is composed of 3 magnets. Each magnet has two stable states showed as *up* and *down* in the figure. We want to switch magnet 2 according to the state of magnet 1. First consider only magnets 1 and 2. We've already explained (see section §I) how magnet 1 can determine the final state of magnet 2. But what happens if more magnets are present?

Consider magnets 1, 2 and 3. Just like magnet 1, magnet 3 also exerts a field on magnet 2 and if it is in the opposite direction can cancel out the field of magnet 1. To overcome this, we apply the pulse to magnet 3 as well thereby diminishing the exerted z field of magnet 3 on magnet 2 so that magnet 1 becomes the sole decider of the final state of magnet 2. In the process the data in magnet 3 has been destroyed (it will end up wherever magnet 4 decides). It takes 3 pulses to transfer the bit (in an inverted manner) in magnet 1 to magnet 4. Magnet 4 has been included because it affects the dissipation of magnet 3 through affecting its dynamics. Inclusion of more magnets to the right or left of the array will not change the quantitative or qualitative results of this paper. Next we'll briefly go over the method used to simulate the chain of inverters.

B. Numerical simulation of the chain of inverters

Equations 13 (with $\alpha = 0.1$) and 14 are used to simulate the dynamics and dissipation of each magnet respectively. The overall scaled (divided by H_c) magnetic field that seats in equation 13 for each magnet at each instant of time now reads

$$\vec{h} = \frac{\vec{H}_{pulse} + \vec{H}_{ani} + \vec{H}_{dip}}{H_c} \quad (15)$$

composed of the applied pulse:

$$\vec{H}_{pulse} = H_{pulse} \hat{y} \quad (16)$$

the anisotropy (internal) field of each magnet:

$$\vec{H}_{ani} = \frac{2Ku_2}{M_s} m_z \hat{z} \quad (17)$$

and exerted dipolar fields of other magnets which in CGS system of units reads

$$\vec{H}_{dip}^j = \sum_{n \neq j} \frac{3(\vec{\mu}_n \cdot \vec{r}_{nj})\vec{r}_{nj} - \vec{\mu}_n r_{nj}^2}{r_{nj}^5} \quad (18)$$

All field values are time dependent. Here j denotes any one magnet and μ_n runs over magnetic moments of the other magnets. Fig.9b shows the LLG simulations of the chain of inverters where magnet 2 is switched solely according to the state of magnet 1 irrespective of its history or the state of magnets 3 and 4.

C. Dissipation of the chain of inverters with one application of the pulse

Fig.9c shows dissipation of the entire array after one application of the pulse as a function of ramp time. The pulse is exerted on magnets 2 and 3 which accounts for the $4Ku_2V$ value in the fast limit. This essentially points out that after cascading these logic building blocks, dissipation changes linearly with the number of magnets.

In the slow limit, depending on the initial configuration, dissipation will be affected. The 4 magnet array can initially be in any of its 16 possible states. Some configurations saturate and some don't. Here the field of magnet 1 plays the role of the bias field H_{dc} for magnet 2 and the field of magnet 4 is like another bias field on magnet 3 which accounts for the 3 groups of curves in Fig.9c. The upper curves correspond to the situation where initial magnetization of both magnets 2 and 3 are opposite to the fields exerted from magnets 1 and 4 respectively. The middle curves correspond to only one of magnets 2 or 3 initially being opposite to the exerted fields of magnet 1 or 4 respectively. The lower curves correspond to both magnets 1 and 3 initially being in the same direction as the exerted fields from magnets 2 and 4 respectively.

An added complication is the field of the other neighbor (magnet 3) which is diminished in the z direction but has a non-negligible y component exerted on magnet 2. All this y directed field does is to wash away a tiny bit the effect of the field of magnet 1 which has little bearing on the qualitative or quantitative results as illustrated in Fig.9c.

VI. DISCUSSION AND PRACTICAL CONSIDERATIONS

A. Dissipation versus speed

The speed of switching can be increased by increasing the magnitude of the external pulse H_{pulse} beyond H_c . Larger fields will dissipate more energy but have the advantage of aligning the magnet faster during the turn-on segment but are of no use for increasing the speed of the turn-off segment because the magnet relaxes to its ground state under its own internal field. If $H_c = \frac{2Ku_2}{M_s}$ can be altered, then it is a better idea to increase H_c and always set $H_{pulse} = H_c$. This way the speed of switching is increased by shortening the time of both turn-on and turn-off segments.

If H_c is increased by increasing Ku_2 (while not changing the volume) then the two methods described above give the same switching energy. This can be seen by comparing equations 3b and 3c where if the $H_{pulse} = H_c$ is increased by the same factor, both equations give the same switching energy. This means that it is more advantageous to increase H_c and set $H_{pulse} = H_c$ to increase switching speed rather than just increasing H_{pulse} beyond H_c . Let's analyze this a little further.

Decreasing M_s results in higher H_c and hence higher speeds with no extra dissipation. However decreasing M_s , decreases the strength of the interaction between the magnetization and the bias field H_{dc} . So for lower M_s , H_{dc} has to be increased in order to have the same amount of guiding control over the switching process. If M_s is held constant, then Ku_2 has to be increased to increase the speed. But an important point is that when Ku_2 is increased, one can lower the volume so that Ku_2V remains constant with the desired retention time and no effect on dissipation. This in turn means that it is possible to increase frequency of operation with no effect on the dissipation per switching event (see Fig.10) which is similar to scalability of CMOS technology where by lowering the capacitance the dissipation per switching event can be held constant at higher switching speeds. This is an important point that is not known offhand when one considers a new device idea. Again we should emphasize that a thorough analysis of external dissipation also has to be done. Next we use these ideas to get some quantitative results.

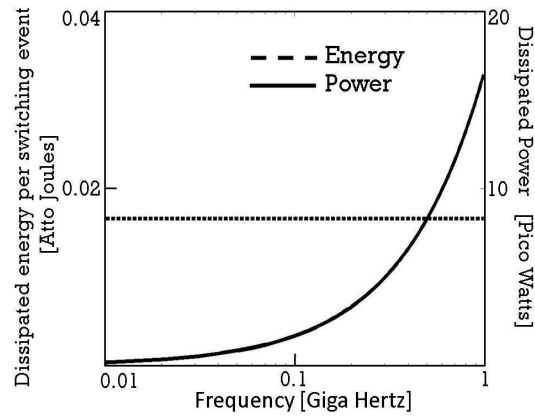


Fig. 10. This figure shows that it is possible to switch magnetic logic bits at higher speeds with the same dissipation (left vertical axes) per switching event similar to CMOS technology. Higher dissipated power (right vertical axes) is only the result of more switching events per unit time. The pulse magnitude (equal to H_c) ranges from ≈ 60 Oe to ≈ 6 KOe.

The barrier height $E_b = Ku_2V$ between the stable states can be engineered by adjusting Ku_2 (anisotropy constant) and V (volume). Considering spherical FePt nanograin alloys, Ku_2 can be made $> 10^7 \text{ erg/cm}^3$ with diameters as low as 4 nm [32]–[34]. Assuming an attempt frequency of $\tau_0^{-1} = 10^{11}$ (this is a conservative estimate; values are usually lower), $Ku_2V \approx 0.5eV$ gives at least a retention time of $1ms$ which allows enough time for computation. The bulk value for saturation magnetization M_s of FePt is 1140 emu/cm^3 . For FePt individual nanograins, M_s depends on annealing temperatures and the types of alloys used and has to be estimated from experiment. Some reported values range from 500 to 900 emu/cm^3 [33]–[35]. Choosing $M_s = 800 \text{ emu/cm}^3$, and $\alpha = 0.1$ which is a typical value for the damping constant, gives us all the relevant parameters. Fig.10 is plotted using these parameter values.

Under the scheme of operation discussed in this paper, with $\tau_r = 2\tau_c$, it takes about $20\tau_c$ to switch a magnet reliably which is used to obtain Fig.10. The applied pulse magnitudes range from $\approx 60\text{Oe}$ to $\approx 6\text{KOe}$ and give the range of frequencies along the horizontal axis. This was obtained by keeping M_s constant and changing the value of Ku_2 thereby changing $H_{pulse} = H_c$ but decreasing the volume by the same factor. The dissipation (vertical axes) already incorporates the significant drop corresponding to ramp times exceeding τ_c given by equation 1. Note that since both cases 1 and 2 (see sections §III-B and §IV) occur in general, the dissipation is the average of these two cases which is the underlying assumption to obtain Fig.10.

B. Integration Density

Integration density is an important issue. Simply stated higher number of devices per unit area will result in higher computational capacity. The low power dissipation of Ferromagnetic bits discussed in the previous sections along with the experimental fact [32] that spherical nano-grain Ferromagnets with diameters in the range of few nanometers can sustain high enough retention times, in principle make it possible to have a high integration density.

Fig.11 shows possibility of tera bit per cm^2 density. This figure is congruent to Fig.10 in that the numerical values of

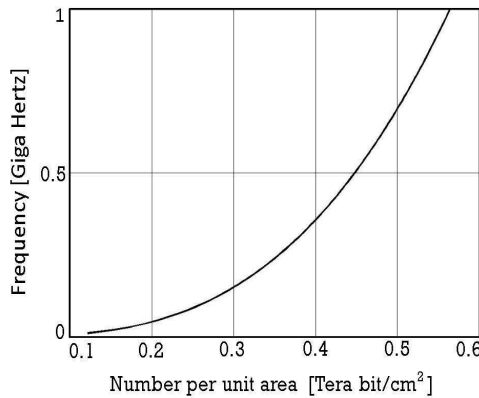


Fig. 11. This figure shows that it is possible to have higher switching frequencies for higher integration densities. It is congruent to Fig.10 in that the dissipation per switching event is constant and has the same numerical value as in Fig.10. These integration densities correspond to spherical nanograins with diameters ranging from $\approx 9\text{nm}$ to $\approx 40\text{nm}$. The diameters have been multiplied by a factor of 20 to get an estimate of the effective area of each device.

volume have been extracted from $Ku_2V = 0.5eV$ for the same range of frequencies as in Fig.10 and that the dissipation of

each switching event remains constant. What is important to realize is that (see Fig.11) higher densities can result in higher switching frequencies similar to CMOS technology. Changing the volume alone does not affect the switching speed; however higher speeds are possible because when the volume is decreased, then Ku_2 can be increased with no extra dissipation; increasing Ku_2 increases speed as discussed earlier. Fig.11 has been obtained by computing the volume of spherical particles and extracting the value of diameter from the volume. That number was then multiplied by a factor of 20 and then it is reported in units of area to account for the spacing between nanomagnets and external circuitry (e.g. wire coil, spin torque, etc) that would provide the pulse.

VII. CONCLUSION

In this paper we analyzed the switching energy of single domain nanomagnets used as cascable logic building blocks. A magnetic pulse was used to provide the energy for switching and a bias field was used as an input to guide the switching. The following conclusions can be drawn from this study.

(1) Through analyzing the complete dependence of the switching energy on ramp time of the pulse, it was concluded that there is a significant and sharp drop in dissipation for ramp times that exceed a critical time given by equation 1 whose significance is separating fast from slow.

(2) The switching energy can be described by a single equation (equation 2) in both fast and slow limits for trapezoidal pulses analyzed in this paper. In the fast limit the effect of the bias field or equivalently the field of neighboring magnet in MQCA systems is negligible so long as the bias field is less than 10th of the switching field of the magnet. In the slow limit however dissipation is largely determined by the value of the bias field.

(3) Quantitative results were provided for dissipated power vs. switching frequency and switching frequency versus integration density. It was concluded that by proper designing, switching energy of Ferromagnetic logic bits can have scaling laws similar to CMOS technology.

(4) By evaluating switching energy of both one magnet and a chain of inverters for MQCA systems, it was shown that the switching energy increases linearly with the number of magnets so that the one magnet results provided in this paper can be used to calculate the switching energy of larger more complicated circuits, at least approximately.

Noise was not directly included in the models; however we took it into account indirectly: thermal noise is the limiting factor on the anisotropy energy Ku_2V of each magnet which we discussed thoroughly. Thermal noise also limits the lowest possible magnitude of the bias field (or equivalently coupling between magnets in MQCA systems). We've provided the results for a wide range of bias values. More thorough discussions of dissipation in the external circuitry can be found in references [13], [14].

REFERENCES

- [1] S. Salahuddin and S. Datta, "Interacting systems for self correcting low power systems", *Appl. Phys. Lett.*, vol.90, pp.093503.1-093503.3, Feb. 2007.
- [2] R.P. Cowburn and M.E. Welland, "Room temperature magnetic quantum cellular automata", *Science*, vol. 287, pp.1466-1468, Feb. 2000.
- [3] R.P. Cowburn, A.O. Adeyeye and M.E. Welland, "Controlling magnetic ordering in coupled nanomagnet arrays", *New J. of Phys.* 1, pp.16.1-16.9, Nov. 1999.
- [4] A.Imre, G. Csaba, L. Ji, A. Orlove, G. H. Bernstein and W. Porod, "Majority Logic Gate for Magnetic Quantum-Dot Cellular Automata", *Science*, vol. 311, pp.205-208, Jan. 2006.
- [5] A. Ney, C. Pampuch, R. Koch and K.H. Ploog, "Programmable computing with a single magnetoresistive element", *Nature*, vol. 425, pp.485-487, Oct. 2003.
- [6] D. A. Allwood, Gang Xiong, M. D. Cooke, C. C. Faulkner, D. Atkinson, N. Vernier and R. P. Cowburn, "Submicrometer Ferromagnetic NOT Gate and Shift Register", *Science*, vol. 296, pp.2003-2004, Jun. 2002.
- [7] D.A. Allwood, G. Xiong, C. C. Faulkner, D. Atkinson, D. Petit and R. P. Cowburn, "Magnetic Domain-Wall Logic", *Science*, vol. 309, pp.1688-1692, Sep. 2002.
- [8] D.E. Nikonov, G.I. Bourianoff, P.A. Gargini, "Simulation of highly idealized, atomic scale MQCA logic circuits", <http://arxiv.org/>, arXiv:0711.2246v1 [cond-mat.mes-hall], Nov. 2007.
- [9] G. Csaba, W. Porod and A. I. Csurgay, "A computing architecture composed of field-coupled single domain nanomagnets clocked by magnetic field", *Int. J. Circ. Theor. Appl.*, vol. 31, pp.67-82, Jan. 2003.
- [10] G. Csaba, A. Imre, G. H. Bernstein, W. Porod and V. Metlushko, "Nanocomputing by field-coupled nanomagnets", *IEEE Trans. on Nanotech.*, vol.1, pp.209-213, Dec. 2002.
- [11] G. Csaba, P. Lugli and W. Porod, "Power dissipation in nanomagnetic logic devices", 4th IEEE Conference on Nanotechnology, pp.346-348, Aug. 2004.
- [12] G. Csaba, P. Lugli, A. Csurgay and W. Porod, "Simulation of power gain and dissipation in field-coupled nanomagnets", *J. Comp. Elec.*, vol. 4, pp.105-110, Aug. 2005.
- [13] M. Niemier, M. Alam, X. S. Hu, G. Bernstein, W. Porod, M. Putney and J. DeAngelis, "Clocking Structures and Power Analysis for Nanomagnet-Based Logic Devices", *Proceedings of the 2007 international symposium on Low power electronics and design (ISLPED)*, New York, ACM, 2007.
- [14] D.E. Nikonov, G.I. Bourianoff and P.A. Gargini, "Power dissipation in spintronic devices out of thermodynamic equilibrium", *J. Super. Novel. Magn.*, vol. 19, No.6, pp. 497-513, Aug. 2006.
- [15] L. Landau and E. Lifshitz, "On the theory of the dispersion of magnetic permeability in ferromagnetic bodies", *Phys. Z. Sowjetunion*, vol. 8, pp.153-169, 1935.
- [16] T.L. Gilbert, "A phenomenological theory of damping in ferromagnetic materials", *IEEE Trans. Magn.*, Vol. 40, pp.3443-3449, Nov. 2004.
- [17] B. Hillebrands (Editor) and K. Ounadjela (Editor), "Spin Dynamics in Confined Magnetic Structures I, II and III", New York, Springer, 2001-2007.
- [18] C.H. Bennet, "The thermodynamics of computation - a review", *Intern. J. Theor. Phys.*, vol. 21, pp. 905-940, Dec. 1982.
- [19] K.K. Likharev and A.N. Korotkov, "Single-electron parametron: reversible computation in a discrete-state system", *Science*, vol. 273, pp. 763-765, Aug. 1996.

- [20] R.K. Kumamuru, A.O. Orlov, R. Ramasubramaniam, C.S. Lent, G.H. Bernstein, and G. Snider, “Operation of a quantum-dot cellular automata (QCA) shift register and analysis of errors”, *IEEE Tran. Elec. Devi.*, Vol.50, pp.1906-1913, Sep. 2003.
- [21] Dissipation in the slow limit depends on the initial direction of the magnetization. If it is opposite to the bias, it saturates to the value described by equation 2. If it is parallel to the bias, it can be made arbitrarily small.
- [22] R. Street and J.C. Woolley, “A Study of Magnetic Viscosity”, *Proc. Phys. Soc., sec. A*, vol. 62, pp.562-572, Sep. 1949.
- [23] L. Neel, “Thermoremanent Magnetization of Fine Powders”, *Rev. Mod. Phys.*, vol. 25, pp. 293 - 295, Jan. 1953.
- [24] W.F. Brown, “Thermal Fluctuations of a Single-Domain Particle”, *Phys. Rev.*, vol. 130, pp.1677-1686, Jun. 1963.
- [25] P. Gaunt, “The frequency constant for thermal activation of a ferromagnetic domain wall”, *J. Appl. Phys.*, vol. 48, pp.3470-3474, Aug. 1977.
- [26] The demagnetizing field or the Weiss field have not been taken into account because they are isotropic for a sphere and can be written as $\lambda\vec{M}$ where \vec{M} is the magnetization. Based on the LLG equation, fields of this form will *not* alter the dynamics of magnetization and has no bearing on dissipation.
- [27] In principle magnet A can switch magnet B unidirectionally with no need for an external pulse given that: $Ku_{2,A}V_A > \frac{(M_{sA}V_A)(M_{sB}V_B)}{7.3} > Ku_{2,B}V_B$ holds. This entails designing circuits with magnets of different parameters (e.g. volume) so no two magnets in the circuit can have the same parameters; not to mention the complexities caused by the fields exerted from other neighbors.
- [28] This essentially states that it is not a matter of principle that interacting magnets must have saturating dissipation as was previously suggested [11]. This is also shown by analyzing the dissipation of a chain of coupled magnets where for some configurations dissipation arbitrarily goes down whereas for some other configurations it saturates. The concepts behind such effects can easily be traced back to the two cases (1 and 2) discussed in the context of one magnet and a bias field H_{dc} .
- [29] R.K. Cavin III, V.V. Zhirmov, J. A. Hutchby, and G. I. Bourianoff, “Energy barriers, demons, and minimum energy operation of electronic devices (Plenary Paper)”, *Proceedings of SPIE*, vol. 5844, pp.1-9, May 2005.
- [30] Z.Z. Sun and X.R. Wang, “Fast magnetization switching of Stoner particles: A nonlinear dynamics picture”, *Phys. Rev. B*, vol. 71, pp. 174430-1 to 174430-9, May 2005.
- [31] Note that the the term $\vec{M} \cdot \frac{d\vec{H}_{applied}}{dt}$ should not have been included in equation 4 of reference 1. However this will not change the results of that paper since this term was assumed to be zero anyways.
- [32] Shouheng Sun, C. B. Murray, D. Weller, L. Folks, and A. Moser, “Monodisperse FePt Nanoparticles and Ferromagnetic FePt Nanocrystal Superlattices”, *Science*, vol. 287, pp.1989-1992, Mar. 2000.
- [33] X.W. Wu, C. Liu, L.Li, P. Jones, R.W. Chantrell and D. Weller, “Nonmagnetic shell in surfactant-coated FePt nanoparticles”, *J. Appl. Phys.*, vol. 95, No.11, pp.6810-6812, Jun. 2004.
- [34] A. Perumal, H.S. Ko and S.C. Shin, “Magnetic properties of carbon-doped FePt nanogranular films”, *Appl. Phys. Lett.*, vol. 83, No.16, pp.3326-3328, Oct. 2003.
- [35] K. Elkins, D. Li, N. Poudyal, V. Nandwana, Z. Jin, K. Chen and J.P. Liu, “Monodisperse face-centered tetragonal FePt nanoparticles with giant coercivity”, *J. Phys. D: Appl. Phys.*, vol. 38, pp.2306-2309, Jul. 2005.
- [36] J.D. Jackson, “Classical Electrodynamics”, New York, Wiley, 1999, pp.198-200.